

# Semiconductor-to-metal transition in bilayer $\text{MoSi}_2\text{N}_4$ and $\text{WSi}_2\text{N}_4$ with strain and electric field

Qingyun Wu,<sup>1, a)</sup> Liemao Cao,<sup>2</sup> Yee Sin Ang,<sup>1</sup> and Lay Kee Ang<sup>1, b)</sup>

<sup>1)</sup> *Science, Mathematics and Technology, Singapore University of Technology and Design (SUTD), 8 Somapah Road, Singapore 487372, Singapore*

<sup>2)</sup> *College of Physics and Electronic Engineering, Hengyang Normal University, Hengyang 421002, China*

With exceptional electrical and mechanical properties and at the same time air-stability, layered  $\text{MoSi}_2\text{N}_4$  has recently draw great attention. However, band structure engineering via strain and electric field, which is vital for practical applications, has not yet been explored. In this work, we show that the biaxial strain and external electric field are effective ways for the band gap engineering of bilayer  $\text{MoSi}_2\text{N}_4$  and  $\text{WSi}_2\text{N}_4$ . It is found that strain can lead to indirect band gap to direct band gap transition. On the other hand, electric field can result in semiconductor to metal transition. Our study provides insights into the band structure engineering of bilayer  $\text{MoSi}_2\text{N}_4$  and  $\text{WSi}_2\text{N}_4$  and would pave the way for its future nanoelectronics and optoelectronics applications.

Since the discovery of graphene,<sup>1-3</sup> there has been great research interests in two-dimensional (2D) layered materials due to their exceptional fundamental physical properties and tremendous potentials in devices applications.<sup>4,5</sup> Owing to their high carrier mobility, excellent on/off ratio and unique optoelectronic properties, 2D transition metal dichalcogenides (TMD)<sup>6-8</sup> and black phosphorene<sup>9-12</sup> have been widely studied in last decade. To fully utilized those semiconducting 2D layered materials in nanoelectronics and optoelectronic devices, band gap engineering is indispensable and plays an essential role in device applications. One of the effective ways of tuning band gap is to apply strain to the layered materials. By doing so, electronic properties of TMD and phosphorene can be altered and strain sensitive device can be designed and fabricated.<sup>13-20</sup> The other strategy to achieve band gap engineering is by applying an external electric field, which may reduce the band gap for bilayer system and even lead to semiconductor to metal transition.<sup>21-29</sup>

Most recently, layered 2D  $\text{MoSi}_2\text{N}_4$  and  $\text{WSi}_2\text{N}_4$  has been experimentally synthesized using chemical vapor deposition (CVD).<sup>30</sup> Experimental results suggest that they have semiconducting characteristic with good mechanical strength and air-stability. The paper also reported an intrinsic electron and hole mobilities of  $270 \text{ cm}^2\text{V}^{-1}\text{s}^{-1}$  and  $1200 \text{ cm}^2\text{V}^{-1}\text{s}^{-1}$ , respectively, for layered 2D  $\text{MoSi}_2\text{N}_4$ , which is around four times as that of  $\text{MoS}_2$ .<sup>30</sup> With higher carrier mobility than  $\text{MoS}_2$  and better air-stability than phosphorene,  $\text{MoSi}_2\text{N}_4$  and its family structure of  $\text{MA}_2\text{Z}_4$  monolayers (M represents an early transition metal, A is Si or Ge, Z stands for N, P or As) have soon received much attention.<sup>31-42</sup> Nevertheless, there is still lack of band gap engineering study of bilayer  $\text{MoSi}_2\text{N}_4$  and  $\text{WSi}_2\text{N}_4$ , which is critical for the future application of layered  $\text{MA}_2\text{Z}_4$  material in nano-

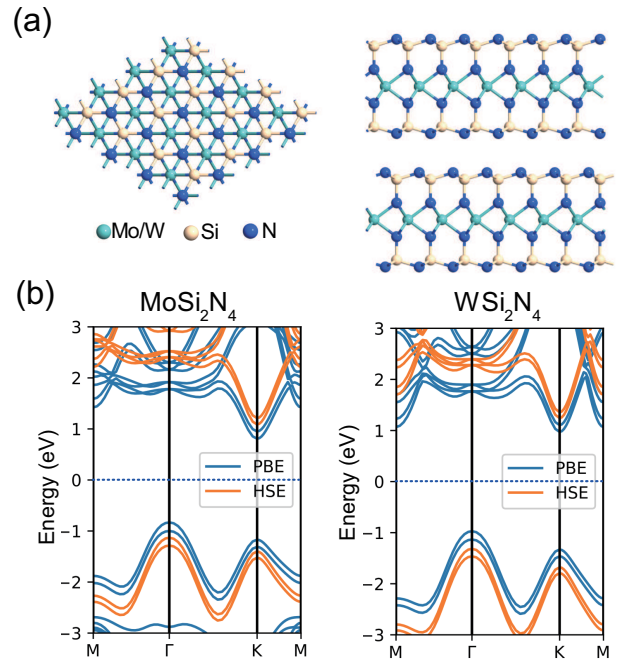


FIG. 1. (a) Top and side view of bilayer  $\text{MoSi}_2\text{N}_4$  and  $\text{WSi}_2\text{N}_4$ . (b) PBE and HSE band structure of bilayer  $\text{MoSi}_2\text{N}_4$  and  $\text{WSi}_2\text{N}_4$ .

electronics and optoelectronic devices up to date.

In this work, we explore the tuning of electrical band structure of bilayer  $\text{MoSi}_2\text{N}_4$  and  $\text{WSi}_2\text{N}_4$  under strain and external electric field. We find that band gaps can be tuned by both compress and tensile strain, which is a result of the change in Mo/W-N bond length and Mo-Mo/W-W distance induced by strain. We also find that the electric field can modulate the band gap, due to the charge redistribution induced by the electric field. Our findings imply that the strain and electric field tunable bilayer  $\text{MoSi}_2\text{N}_4$  and  $\text{WSi}_2\text{N}_4$  could be promising materials for the next generation nanoelectronics and optoelectronics.

<sup>a)</sup> Electronic mail: [qingyun\\_wu@sutd.edu.sg](mailto:qingyun_wu@sutd.edu.sg)

<sup>b)</sup> Electronic mail: [ricky\\_ang@sutd.edu.sg](mailto:ricky_ang@sutd.edu.sg)

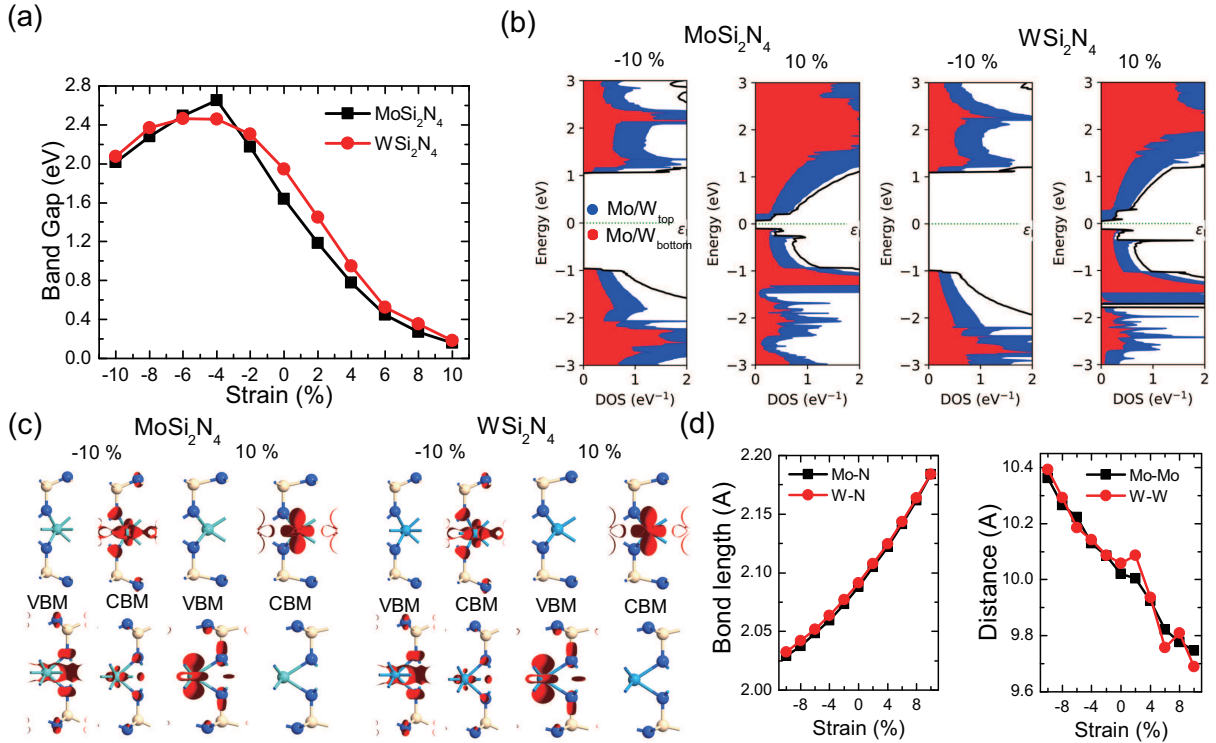


FIG. 2. (a) Band gap as a function of applied strain for bilayer MoSi<sub>2</sub>N<sub>4</sub>/WSi<sub>2</sub>N<sub>4</sub>. (b) Projected density of states (PDOS) for bilayer MoSi<sub>2</sub>N<sub>4</sub> and WSi<sub>2</sub>N<sub>4</sub> under -10 % and 10 % strain. (c) Partial charge density corresponding to the valence band maximum (VBM) and conduction band minimum (CBM) for bilayer MoSi<sub>2</sub>N<sub>4</sub> and WSi<sub>2</sub>N<sub>4</sub> under -10 % and 10 % strain. (d) Mo-N/W-N bond length and Mo-Mo/W-W distance as a function of applied strain for bilayer MoSi<sub>2</sub>N<sub>4</sub> and WSi<sub>2</sub>N<sub>4</sub>.

Our first-principles study is carried out based on the density functional theory (DFT) calculations. The Vienna *Ab initio* Simulation Package (VASP)<sup>43,44</sup> was adopted for the geometry optimization and the QuantumATK<sup>45</sup> was used to investigate the electronic properties of bilayer MoSi<sub>2</sub>N<sub>4</sub> and WSi<sub>2</sub>N<sub>4</sub> under strain and external electric field. A gamma-centered Brillouin zone  $k$ -point sampling grid using the Monkhorst-Pack method<sup>46</sup> of  $9 \times 9 \times 1$  was used for geometry optimization and a grid of  $15 \times 15 \times 1$  for property calculations. Atomic geometry optimization criteria is that all forces are smaller than  $0.01 \text{ eV}/\text{\AA}$ . The generalized gradient approximation (GGA) with the Perdew-Burke-Ernzerhof form (PBE)<sup>47</sup> was chosen for the exchange-correlation functional in the calculations. The Heyd-Scuseria-Ernzerhof hybrid functional method (HSE)<sup>48</sup> was also used to obtain the more accurate band structure of the bilayers. To take into account the weak van der Waals interactions in the bilayers, we adopted the DFT-D3 method with the Grimme scheme<sup>49,50</sup> in the calculations. A  $20 \text{ \AA}$  thick of vacuum layer was inserted between adjacent bilayers to eliminate the interactions from periodic images.<sup>51</sup>

Based on our total energy calculations and also previous results,<sup>30</sup> the AC stacking of the bilayer MoSi<sub>2</sub>N<sub>4</sub> and WSi<sub>2</sub>N<sub>4</sub> is the most stable bilayer configuration with the

lowest total energy. Therefore, we only focus on the AC stacking in the following discussions. Figure 1(a) depicts the optimized geometric structure of the bilayer MoSi<sub>2</sub>N<sub>4</sub> and WSi<sub>2</sub>N<sub>4</sub>. Our calculated lattice parameter of the bilayer MoSi<sub>2</sub>N<sub>4</sub> and WSi<sub>2</sub>N<sub>4</sub> is  $a = 2.90/2.90 \text{ \AA}$ , which is in good agreement with previous calculated results.<sup>30</sup> As shown in Fig. 1(b) the band structure of the bilayer MoSi<sub>2</sub>N<sub>4</sub> and WSi<sub>2</sub>N<sub>4</sub> is very similar to its monolayer counterpart with only small splitting in energy bands induced by the interlayer interactions, which slightly reduces the band gap. The indirect band gap of the bilayer MoSi<sub>2</sub>N<sub>4</sub> and WSi<sub>2</sub>N<sub>4</sub> is calculated to be  $1.64/1.94 \text{ eV}$ . To obtain a more accurate band structure, the HSE hybrid functional calculations were also performed. It is found that the shape of the HSE bands are similar to that of the PBE results with only valence bands pushed down and conduction bands pushed up. We obtain the band gap value of  $2.22/2.56 \text{ eV}$  for the bilayer MoSi<sub>2</sub>N<sub>4</sub> and WSi<sub>2</sub>N<sub>4</sub> in HSE calculations.

It has been proved that strain engineering is an effective avenue to modulate the electric, magnetic and optical properties of 2D layered materials. To understand the tunability of the energy band gap of the bilayer MoSi<sub>2</sub>N<sub>4</sub> and WSi<sub>2</sub>N<sub>4</sub>, we applied biaxial strain to the system. The strain ( $\varepsilon$ ) is evaluated using  $\varepsilon = (a - a_0)/a_0 \times 100\%$ , where  $a$  and  $a_0$  are the lattice parameter of the strained

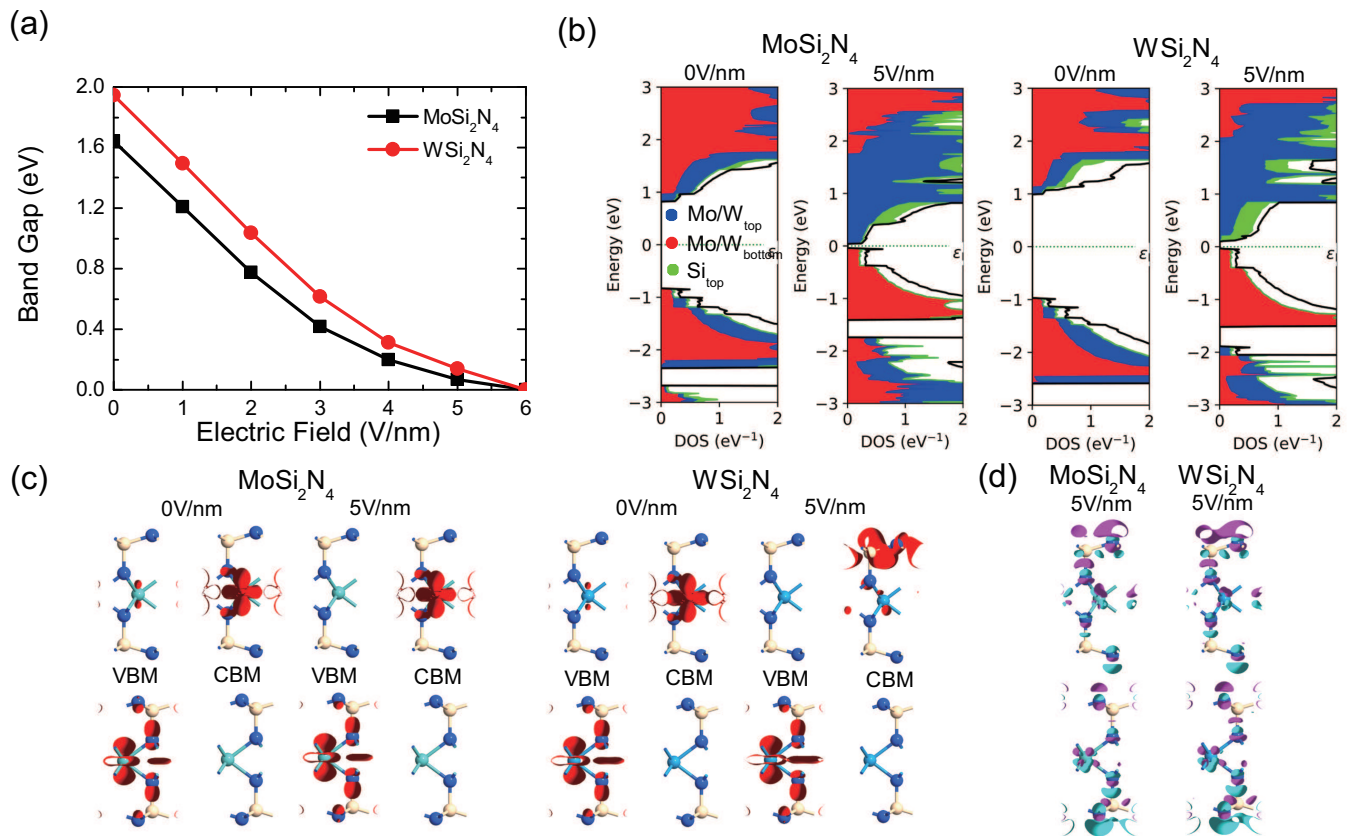


FIG. 3. (a) Band gap as a function of applied electric field for bilayer MoSi<sub>2</sub>N<sub>4</sub> and WSi<sub>2</sub>N<sub>4</sub>. (b) Projected density of states (PDOS) for bilayer MoSi<sub>2</sub>N<sub>4</sub> and WSi<sub>2</sub>N<sub>4</sub> under 0 V/nm and 5 V/nm electric field. (c) Partial charge density corresponding to the valance band maximum (VBM) and conduction band minimum (CBM) for bilayer MoSi<sub>2</sub>N<sub>4</sub>/WSi<sub>2</sub>N<sub>4</sub> under 0 V/nm and 5 V/nm electric field. (d) Charge redistribution for bilayer MoSi<sub>2</sub>N<sub>4</sub> and WSi<sub>2</sub>N<sub>4</sub> under 5 V/nm electric field. The blue (red) isosurfaces represent charge accumulation (depletion).

and unstrained bilayer, respectively. Figure 2(a) shows the evolution of the band gap as a function of applied strain for bilayer MoSi<sub>2</sub>N<sub>4</sub> and WSi<sub>2</sub>N<sub>4</sub>. It is suggested that the band gap undergoes a monotonous decreasing with the increasing tensile strain. However, with increasing compress strain, the band gap increases then decreases at around -4 % for the bilayer MoSi<sub>2</sub>N<sub>4</sub> and -6 % for the bilayer WSi<sub>2</sub>N<sub>4</sub>. Besides varying the band gap, more importantly, strain is also found to change an indirect band gap semiconductor to a direct band gap semiconductor at about -4 % of compress strain for the bilayer MoSi<sub>2</sub>N<sub>4</sub>. (See Fig. S1) To understand the electronic structure engineering by strain, we draw the projected density of states (PDOS) and partial charge density corresponding to the valance band maximum (VBM) and conduction band minimum (CBM) for bilayer MoSi<sub>2</sub>N<sub>4</sub> and WSi<sub>2</sub>N<sub>4</sub> under -10 % and 10 % strain in Fig. 2(b) and Fig. 2(c). As can be seen from the figure, the VBM and CBM are mostly contributed from both the metal atoms of the top and bottom layer of the bilayer with an enlarged band gap for the compress -10 % strain in the PDOS. In the partial charge density plot, we see more  $d_{xy}$  and  $d_{x^2-y^2}$  orbitals for the metal atoms in VBM

and CBM for the compress -10 % strain. This is because the  $d_{xy}$  and  $d_{x^2-y^2}$  orbitals are favorable for the in-plane bonding. The reduced bond length of Mo/W-N under compress strain facilitate the in-plane bonding, as shown in Fig. 2(d). The VBM is mostly from the Mo/W atom of the bottom layer and the CBM is mostly from the Mo/W atom of the top layer, respectively, with a reduced band gap for the tensile 10 % strain. This split of the VBM and CBM from the metal atoms of the two different layer can be understood from the shorten distance of two metal atoms which increases the interlayer interactions as shown in Fig. 2(d). Different from the compressed case, we see more  $d_{z^2}$  orbitals for the metal atoms in VBM and CBM for the tensile 10 % strain. This is because the  $d_{z^2}$  orbital is favorable for the out-of-plane bonding. When the bond length increase, the out-of-plane bonding become more significant and thus more  $d_{z^2}$  orbitals.

Applying an external electric field perpendicular to the layered material is another effective way of tuning the properties of 2D layered materials. The evolution of the band gap as a function of the applied electric field for bilayer MoSi<sub>2</sub>N<sub>4</sub> and WSi<sub>2</sub>N<sub>4</sub> is provided in Fig. 3(a). It



is found that the band gap decreases monotonously with the increasing electric field and closes at 6 V/nm for both bilayer MoSi<sub>2</sub>N<sub>4</sub> and WSi<sub>2</sub>N<sub>4</sub>. It is also interesting to find that the CBM for MoSi<sub>2</sub>N<sub>4</sub> is at the K point while the CBM for WSi<sub>2</sub>N<sub>4</sub> moves to the M point when the band gap closes. (See Fig. S2) To gain more insight to the electronic structure engineering by electric field, we plot the PDOS and partial charge density of VBM and CBM for bilayer MoSi<sub>2</sub>N<sub>4</sub> and WSi<sub>2</sub>N<sub>4</sub> under 0 V/nm and 5 V/nm electric field in Fig. 3(b) and Fig. 3(c). As can be seen from the figure, the overall shape of the PDOS of the bottom and top metal atoms almost remain the same under 5V/nm electric field. However, the energy bands of the bottom metal atom shift up while the energy bands of the up atom shift down, which gradually closes the band gap. Furthermore, the CBM of the bilayer WSi<sub>2</sub>N<sub>4</sub> under 5V/nm electric field comes from the top Si atom that can be observed both from the PDOS and the partial charge density plot. This explains why the CBM for WSi<sub>2</sub>N<sub>4</sub> moves to the M point under 5V/nm electric field. This band gap engineering by external electric field can be interpreted from the charge redistribution of the bilayer MoSi<sub>2</sub>N<sub>4</sub> and WSi<sub>2</sub>N<sub>4</sub> under electric field as shown in Fig. 3(d). The charge density difference ( $\Delta\rho$ ) is defined as  $\Delta\rho = \rho_E - \rho_0$  where  $\rho_E$  and  $\rho_0$  are the charge densities of the bilayer MoSi<sub>2</sub>N<sub>4</sub> and WSi<sub>2</sub>N<sub>4</sub> with and without the external electric field, respectively. Here, positive (negative)  $\Delta\rho$  indicates charge accumulation (depletion). As can be seen from the figure, there is charge accumulation in the bottom layer and depletion in the top layer. This leads to the VBM in the bottom layer shifting up and the CBM in the top layer shifting down, which reduces the energy band gap.

In conclusion, we have shown that the biaxial strain and external electric field are effective ways for the band gap engineering of bilayer MoSi<sub>2</sub>N<sub>4</sub> and WSi<sub>2</sub>N<sub>4</sub>. Band gaps can be tuned by both compress and tensile strain. Compress strain can even leads to indirect band gap to direct band gap transition. The change in Mo/W-N bond length and Mo-Mo/W-W distance induced by strain is the main reason for this band structure engineering. Electric field can also modulate the band gap and even semiconductor to metal transition. Charge redistribution induced by the electric field accounts for the band gap tuning. Our study suggests the strain and electric field tunable bilayer MoSi<sub>2</sub>N<sub>4</sub> and WSi<sub>2</sub>N<sub>4</sub> could be promising materials for the next generation nanoelectronics and optoelectronics.

This work is supported by Singapore MOE Tier 2 (Grant No. 2018-T2-1-007). All the calculations were carried out using the computational resources provided by the National Supercomputing Centre (NSCC) Singapore.

### Data Availability

The data that support the findings of this study are available from the corresponding author upon reasonable request.

- <sup>1</sup>K. S. Novoselov, A. K. Geim, S. V. Morozov, D. Jiang, Y. Zhang, S. V. Dubonos, I. V. Grigorieva, and A. A. Firsov, *Science* **306**, 666 (2004).
- <sup>2</sup>K. S. Novoselov, D. Jiang, F. Schedin, T. Booth, V. Khotkevich, S. Morozov, and A. K. Geim, *Proc. Natl. Acad. Sci. U.S.A.* **102**, 10451 (2005).
- <sup>3</sup>K. S. Novoselov, A. K. Geim, S. V. Morozov, D. Jiang, M. I. Katsnelson, I. V. Grigorieva, S. V. Dubonos, and A. A. Firsov, *Nature* **438**, 197 (2005).
- <sup>4</sup>G. R. Bhimanapati, Z. Lin, V. Meunier, Y. Jung, J. Cha, S. Das, D. Xiao, Y. Son, M. S. Strano, V. R. Cooper, *et al.*, *ACS Nano* **9**, 11509 (2015).
- <sup>5</sup>C. Tan, X. Cao, X.-J. Wu, Q. He, J. Yang, X. Zhang, J. Chen, W. Zhao, S. Han, G.-H. Nam, *et al.*, *Chem. Rev.* **117**, 6225 (2017).
- <sup>6</sup>K. F. Mak, C. Lee, J. Hone, J. Shan, and T. F. Heinz, *Phys. Rev. Lett.* **105**, 136805 (2010).
- <sup>7</sup>B. Radisavljevic, A. Radenovic, J. Brivio, V. Giacometti, and A. Kis, *Nat. Nanotechnol.* **6**, 147 (2011).
- <sup>8</sup>A. Splendiani, L. Sun, Y. Zhang, T. Li, J. Kim, C.-Y. Chim, G. Galli, and F. Wang, *Nano Lett.* **10**, 1271 (2010).
- <sup>9</sup>H. Liu, A. T. Neal, Z. Zhu, Z. Luo, X. Xu, D. Tománek, and P. D. Ye, *ACS Nano* **8**, 4033 (2014).
- <sup>10</sup>L. Li, Y. Yu, G. J. Ye, Q. Ge, X. Ou, H. Wu, D. Feng, X. H. Chen, and Y. Zhang, *Nat. Nanotechnol.* **9**, 372 (2014).
- <sup>11</sup>S. P. Koenig, R. A. Doganov, H. Schmidt, A. Castro Neto, and B. Özyilmaz, *Appl. Phys. Lett.* **104**, 103106 (2014).
- <sup>12</sup>J. Qiao, X. Kong, Z.-X. Hu, F. Yang, and W. Ji, *Nat. Commun.* **5**, 1 (2014).
- <sup>13</sup>P. Johari and V. B. Shenoy, *ACS Nano* **6**, 5449 (2012).
- <sup>14</sup>W. S. Yun, S. Han, S. C. Hong, I. G. Kim, and J. Lee, *Phys. Rev. B* **85**, 033305 (2012).
- <sup>15</sup>S. Bhattacharyya and A. K. Singh, *Phys. Rev. B* **86**, 075454 (2012).
- <sup>16</sup>H. Pan and Y.-W. Zhang, *J. Phys. Chem. C* **116**, 11752 (2012).
- <sup>17</sup>H. Guo, N. Lu, J. Dai, X. Wu, and X. C. Zeng, *J. Phys. Chem. C* **118**, 14051 (2014).
- <sup>18</sup>A. Rodin, A. Carvalho, and A. C. Neto, *Phys. Rev. Lett.* **112**, 176801 (2014).
- <sup>19</sup>X. Peng, Q. Wei, and A. Copple, *Phys. Rev. B* **90**, 085402 (2014).
- <sup>20</sup>R. Fei and L. Yang, *Nano Lett.* **14**, 2884 (2014).
- <sup>21</sup>A. Ramasubramaniam, D. Naveh, and E. Towe, *Phys. Rev. B* **84**, 205325 (2011).
- <sup>22</sup>Q. Liu, L. Li, Y. Li, Z. Gao, Z. Chen, and J. Lu, *J. Phys. Chem. C* **116**, 21556 (2012).
- <sup>23</sup>T. Chu, H. Ilatikhameneh, G. Klimeck, R. Rahman, and Z. Chen, *Nano Lett.* **15**, 8000 (2015).
- <sup>24</sup>K. Dolui, C. D. Pemmaraju, and S. Sanvito, *ACS Nano* **6**, 4823 (2012).
- <sup>25</sup>L. Kou, C. Tang, Y. Zhang, T. Heine, C. Chen, and T. Frauenheim, *J. Phys. Chem. Lett.* **3**, 2934 (2012).
- <sup>26</sup>Q. Liu, X. Zhang, L. Abdalla, A. Fazzio, and A. Zunger, *Nano Lett.* **15**, 1222 (2015).
- <sup>27</sup>Q. Wu, L. Shen, M. Yang, Y. Cai, Z. Huang, Y. P. Feng, *et al.*, *Phys. Rev. B* **92**, 035436 (2015).
- <sup>28</sup>L. Huang, N. Huo, Y. Li, H. Chen, J. Yang, Z. Wei, J. Li, and S.-S. Li, *J. Phys. Chem. Lett.* **6**, 2483 (2015).
- <sup>29</sup>L. Cao, Y. S. Ang, Q. Wu, and L. Ang, *Appl. Phys. Lett.* **115**, 241601 (2019).
- <sup>30</sup>Y.-L. Hong, Z. Liu, L. Wang, T. Zhou, W. Ma, C. Xu, S. Feng, L. Chen, M.-L. Chen, D.-M. Sun, *et al.*, *Science* **369**, 670 (2020).
- <sup>31</sup>K. S. Novoselov, *Natl. Sci. Rev.* **7**, 1842 (2020).
- <sup>32</sup>L. Tang, J. Tan, H. Nong, B. Liu, and H.-M. Cheng, *Acc. Mater. Res.* (2020).
- <sup>33</sup>S. Li, W. Wu, X. Feng, S. Guan, W. Feng, Y. Yao, and S. A. Yang, *Phys. Rev. B* **102**, 235435 (2020).
- <sup>34</sup>L. Cao, G. Zhou, Q. Wang, L. Ang, and Y. S. Ang, *Appl. Phys. Lett.* **118**, 013106 (2021).
- <sup>35</sup>S.-D. Guo, W.-Q. Mu, Y.-T. Zhu, and X.-Q. Chen,

- Phys. Chem. Chem. Phys.* **22**, 28359 (2020).
- <sup>36</sup>S.-D. Guo, Y.-T. Zhu, W.-Q. Mu, and W.-C. Ren, *Europhys. Lett.* **132**, 57002 (2020).
- <sup>37</sup>B. Mortazavi, B. Javvaji, F. Shojaei, T. Rabczuk, A. V. Shapeev, and X. Zhuang, *Nano Energy* **82**, 105716 (2020).
- <sup>38</sup>A. Bafekry, M. Faraji, D. M. Hoat, M. Fadlallah, M. Shahrokhi, F. Shojaei, D. Gogova, and M. Ghergherehchi, [arXiv:2009.04267](https://arxiv.org/abs/2009.04267) (2020).
- <sup>39</sup>C. Yang, Z. Song, X. Sun, and J. Lu, [arXiv:2010.10764](https://arxiv.org/abs/2010.10764) (2020).
- <sup>40</sup>J. Yu, J. Zhou, X. Wan, and Q. Li, [arXiv:2012.14120](https://arxiv.org/abs/2012.14120) (2020).
- <sup>41</sup>L. Kang and Z. Lin, [arXiv:2009.06977](https://arxiv.org/abs/2009.06977) (2020).
- <sup>42</sup>Q. Wang, L. Cao, S.-J. Liang, W. Wu, G. Wang, C. H. Lee, W. L. Ong, H. Y. Yang, L. K. Ang, S. A. Yang, *et al.*, [arXiv:2012.07465](https://arxiv.org/abs/2012.07465) (2020).
- <sup>43</sup>G. Kresse and J. Furthmüller, *Phys. Rev. B* **54**, 11169 (1996).
- <sup>44</sup>G. Kresse and J. Furthmüller, *Comput. Mater. Sci.* **6**, 15 (1996).
- <sup>45</sup>S. Smidstrup, T. Markussen, P. Vancraeyveld, J. Wellendorff, J. Schneider, T. Gunst, B. Verstichel, D. Stradi, P. A. Khomyakov, U. G. Vej-Hansen, *et al.*, *J. Phys.: Condens. Matter* **32**, 015901 (2019).
- <sup>46</sup>H. J. Monkhorst and J. D. Pack, *Phys. Rev. B* **13**, 5188 (1976).
- <sup>47</sup>J. P. Perdew, K. Burke, and M. Ernzerhof, *Phys. Rev. Lett.* **77**, 3865 (1996).
- <sup>48</sup>J. Heyd, G. E. Scuseria, and M. Ernzerhof, *J. Chem. Phys.* **118**, 8207 (2003).
- <sup>49</sup>S. Grimme, J. Antony, S. Ehrlich, and H. Krieg, *J. Chem. Phys.* **132**, 154104 (2010).
- <sup>50</sup>S. Grimme, S. Ehrlich, and L. Goerigk, *J. Comput. Chem.* **32**, 1456 (2011).
- <sup>51</sup>Q. Wu, Y. S. Ang, L. Cao, and L. K. Ang, *Appl. Phys. Lett.* **115**, 083105 (2019).